

A. P. Bedin, I. M. Dement'ev, and G. I. Mishin

Zhurnal Prikladnoi Mekhaniki i Tekhnicheskoi Fiziki, Vol. 9, No. 2, pp. 95-98, 1968

The effect of Reynolds number on the geometric characteristics of flow under conditions of boundary layer separation from the surface of a sphere is analyzed.

The point of boundary layer separation is determined.

The angle between the tangent to the surface of the sphere at the point of its intersection with the extension of the shock wave and the tangent to the separation surface is defined.

Measurements were made of the angle between the visible separation boundary and the compression jump developing in the neighborhood of the separation point.

NOTATION

- p is the pressure;
- ρ is the density;
- t is the temperature;
- V_∞ is the velocity of model;
- d is the diameter of the model;
- M is the Mach number;
- R is the Reynolds number;

γ is the coordinate of the point of intersection of the shock-wave continuation and the sphere surface, with the superscript $^\circ$ denoting measured values;

γ_1 is the coordinate of the point of intersection of the continuation of the edge of the separated boundary layer and the sphere surface;

ψ is the angle between the shock wave and the tangent to the separation boundary;

φ is the angle between the tangent to the separation boundary and the direction of flight of the model;

β is the angle between the tangent to the surface of the sphere (at its point of intersection with the shock-wave continuation) and the tangent to the separation surface;

L is the distance between the point of separation of the boundary layer and the loss-of-stability point of the laminar flow in the wake;

δ is the separation of the head shock wave from the sphere.

Shadographs of flow past a sphere (1:1) obtained in ballistic wind tunnels [1,2] were used for measuring the flow separation and the head-wave detachment.

The experiments were carried out in air ($t \sim 17^\circ \text{C}$) at atmospheric and reduced pressure in the range of Mach numbers 0.8-4.0.

Duralumin balls (class 10 surface finish) of 53, 39, 30, and 20 mm in diameter and 9mm steel ball bearings (class 11 surface finish) were fired at atmospheric pressure. These steel balls were also fired at a pressure p of approximately 190 mm Hg in the ballistic wind tunnel.

The Reynolds number R varied in these experiments between $6 \cdot 10^4$ and $4.6 \cdot 10^6$ in proportion to the flight velocity.

The effect of surface roughness was investigated during experiments carried out in air at atmospheric pressure with 20 mm diameter steel ball (class 11 surface finish), and rough-finished duralumin balls of the same diameter. Surface roughness (0.03 mm ridge height) was produced by sandblasting.

The refraction of light rays at compression jumps and in boundary layers produces areas of shadow whose cross section is observed on the screen in the form of black strips (the pattern of rays, shown schematically in Fig. 1, relates to the case of an abrupt change of density ρ at the edge of the boundary layer and in the shock wave). The rays tangent to the shock wave or to the boundary layer edge, intersecting with the screen, are the external boundaries of these strips and were used for all measurements.

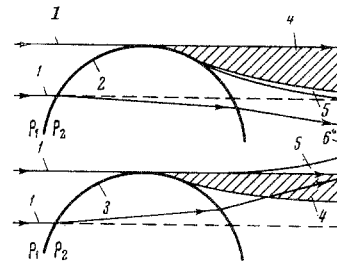


Fig. 1. 1) Light rays; 2) shock wave ($\rho_1 < \rho_2$); 3) edge of the boundary layer ($\rho_1 > \rho_2$); 4) region of shadow; 5) region of highlight; 6) screen.

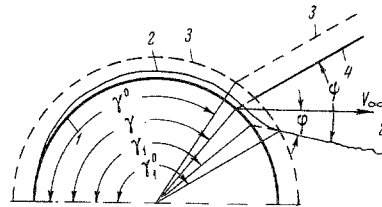


Fig. 2. 1) Sphere; 2) edge of the boundary layer; 3) diffraction edge; 4) compression jump.

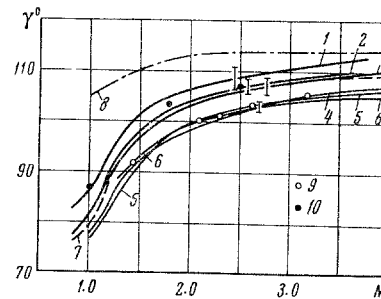


Fig. 3. 1) $d = 53$ mm; 2) $d = 39$ mm; 3) $d = 30$ mm; 4) $d = 20$ mm; 5) $d = 9$ mm, 6) $p = 190$ mm Hg; 7) $d = 14.2$ mm [4]; 8) calculated, $R = 10^7$ [3]; 9) $d = 20$ mm (class 11 surface finish); 10) $d = 20$ mm (rough surface).

Since, owing to diffraction, the position of the shadow-light boundary is displaced, the results of the measurements were corrected for this effect. Two corrections, $\Delta_1 \gamma$ and $\Delta_2 \gamma$, were made with respect to angle γ (Fig. 2) which defines the position of the intersection point of the sphere surface and the continuation of the shock wave originating in the separation zone (the first of these takes into account the presence of the model diffraction edge and the second, that at the shock wave), thus $\gamma = \gamma^\circ - \Delta_1 \gamma + \Delta_2 \gamma$. The experimentally obtained dependence of the parameter γ° on the Mach number M for balls of various diameters is shown in Fig. 3. Each of the curves plotted on this graph is the result of averaging of not less than 100 points. The graph shows the mean deviation of individual measurements of γ° for each curve. Values related to rough-finished balls and to 20 mm diameter

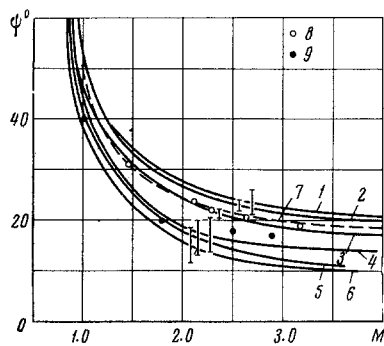


Fig. 4. 1) $d = 9$ mm, $p = 190$ mm Hg; 2) $d = 9$ mm; 3) $d = 20$ mm; 4) $d = 30$ mm; 5) $d = 39$ mm; 6) $d = 53$ mm; 7) $d = 14.2$ mm [4]; 8) $d = 20$ mm (class 11 surface finish); 9) $d = 20$ mm (rough surface).

balls (class 11 surface finish) are mean values obtained from the processing of some 20 exposures. It will be seen from this graph that for balls of diameters $d \leq 20$ mm the dependence of γ on the Mach number is practically the same. For balls of larger diameters ($d > 20$ mm) the point of boundary layer separation moves downstream. Surface roughness has a similar effect on it.

The quantitative discrepancy between values of γ calculated for $R = 10^7$ [3] and those obtained in the course of the present experiments at the upper limit of the investigated range of Reynolds numbers $R = 4.6 \cdot 10^6$ is not great. The discrepancy between values of γ determined here and those determined in [4] can be explained by the fact that in the latter no corrections were made for diffraction edges at the ball and at the compression jump.

The results of measurements of angles ψ (between the tangent to the separation boundary and the shock wave) and φ (between the same tangent and the model's direction of flight) are shown in Figs. 4 and 5 in graph form of functions $\psi = \psi(M)$ and $\varphi = \varphi(M)$. Data from [4] have been also plotted on these diagrams and are in good correlation with the results of this investigation.

The set of relationships $\gamma = \gamma(M)$ and $\varphi = \varphi(M)$ (Figs. 3 and 5) allow us to calculate the angle β between the tangent to the sphere at the point of its intersection with the shock wave continuation and the tangent to the surface of separation (in rough approximation, β may be identified with the deflection angle of the stream in the separation zone). The results of calculations made for several values of the Mach number M are given, in Fig. 6, in the form of curves of $\beta = \beta(R)$. The

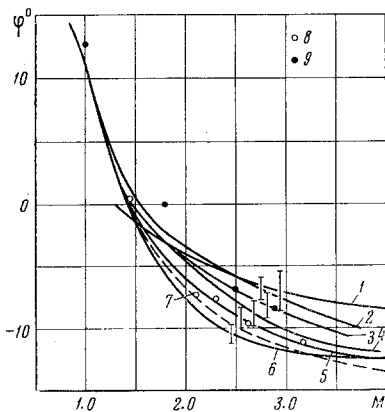


Fig. 5. 1) $d = 9$ mm, $p = 190$ mm Hg; 2) $d = 53$ mm; 3) $d = 39$ mm; 4) $d = 30$ mm; 5) $d = 20$ mm; 6) $d = 9$ mm; 7) $d = 14.2$ mm [4]; 8) $d = 20$ mm (Class 11 surface finish); 9) $d = 20$ mm (rough surface).

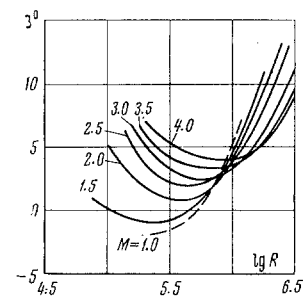


Fig. 6. Dependence of β on the Reynolds number for various Mach numbers.

presence of a minimum whose magnitude and position varies with a varying Mach number M is a particular characteristic of these curves.

An examination of Fig. 6 shows that, in a number of cases, angle β is negative. This may be explained by the fact that the flow separation beginning at the point defined by coordinate γ , is not abrupt but gradual. It will readily be seen that, for separations of this nature, the point of intersection of the continuation of the upper boundary of the separated boundary layer with the surface of the sphere (γ_1 in Fig. 2) may appear behind the point of intersection of the shock wave with the ball (γ). Direct measurements of the position of these points on the sphere showed that for $R < 5 \cdot 10^5$, $\gamma_1 > \gamma$, and the difference $\gamma_1 - \gamma \approx 10^\circ$, while for $R > 5 \cdot 10^5$, the latter is 4° . It should be noted, as regards parameter γ_1 , that only one correction, $\Delta_1 \gamma_1$ (Fig. 2), for the model diffraction edge was made.

The obtained data allow us to make certain observations as regards the dependence of the pressure aft of the sphere on R . In particular, since γ ($d \leq 20$ mm) is nearly constant for decreasing Reynolds numbers (Fig. 3) and since the angle of stream deflection increases (Fig. 6), the pressure behind the compression jump increases. Hence, in this region the ratio of the back pressure to the pressure at infinity increases with decreasing Reynolds number. At Reynolds numbers $R < 5 \cdot 10^5$, the zone of deflection of a stream detached from the sphere surface (roughly characterized by the parameter $\gamma_1 - \gamma$) is greater than for $R > 5 \cdot 10^5$. Thus, the rise of pressure behind a compression jump at "low" Reynolds numbers will be slower than at "high" numbers.

Light rays intersecting the region of turbulent flow deviate from their original path (owing to density pulsation in the flow) thus making local inhomogeneities of flow visible. This feature was used for determining the position of the "point" of transition from laminar to turbulent flow. It was assumed in these measurements that the loss of the laminar flow stability occurs at the instant of appearance on the shadowgraph of local inhomogeneities in the illuminated field. Results of measurements are shown in Fig. 7 in the form of a graph showing the dependence of parameter $l = l/d$ on the Mach number M . Here L is the distance between the intersection point of the shock-wave

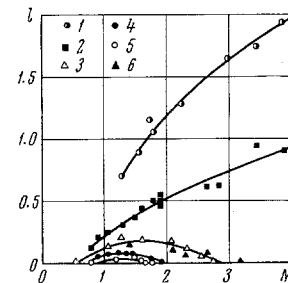


Fig. 7. 1) $d = 9$ mm, $p = 190$ mm Hg; 2) $d = 9$ mm; 3) $d = 20$ mm; 4) $d = 30$ mm; 5) $d = 39$ mm; 6) $d = 20$ mm (class 11 surface finish).

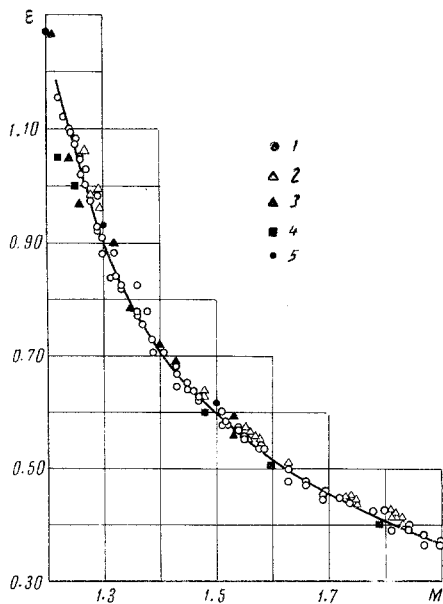


Fig. 8. 1) Air, $p = 1$ atm; $d = 20$ mm, dural; 2) air, $p = 190$ mm Hg; $d = 9$ mm, steel; 3) nitrogen, $c_p/c_v = 1.4$ [5]; 4) air [6]; 5) calculated, $c_p/c_v = 1.4$ [7].

continuation and the sphere and the spot at which the first visible inhomogeneities of flow make their appearance. Each point on the graph represents the value of l determined by averaging measurements made on a series of exposures taken in the course of a single experiment. Examination of this graph shows that the transition from laminar to turbulent flow is retarded in the wake with increasing Mach number M (curves relate to a 9 mm diameter sphere). This is explained by the greater stability of the boundary layer at high Mach numbers M than at low ones. A decrease of the Reynolds number (at constant Mach number M) results in a downstream shift of the transition point. However, no stretches of laminar flow behind the overcompression region were detected in the wake during the course of these experiments, since the over compression region moves in the same direction.

Results of measurements of the relative separation of the shock wave $\epsilon = 2\delta/d$ as a function of the Mach number are shown in Fig. 8, where, for comparison, data from [5-7] have also been included. The results of this investigation and those of [5] are in good correlation, although yielding higher values for ϵ than those quoted in [6]. The calculated values adduced in [7] lie somewhat higher than those of the present experiments. This discrepancy may be explained by the high deceleration to which a model is subjected in conditions of ballistic experiments. Under such circumstances the shock-wave detachment is increased.

In conclusion, the authors express their gratitude to A. A. Sokolov and I. I. Skovortsov for their participation in these experiments.

REFERENCES

1. G. I. Mishin and N. P. Mende, "Sealed ballistic range," collection: Aerophysical Investigation of Supersonic Flows [in Russian], Yu. A. Dunaev, ed., Izd-vo Nauka, 1967.
2. I. V. Basargin, I. M. Dement'ev, and G. I. Mishin, "Range for aerodynamic investigations," collection: Aerophysical Investigations of Supersonic Flows [in Russian], Yu. A. Dunaev, ed., Izd-vo Nauka, 1967.
3. M. Ya. Yudelovich, "An approximate method for calculating the pressure aft of spheres" *Izv. AN SSSR, Mekhanika*, no. 3, 1965.
4. A. C. Charters and R. N. Thomas, "The aerodynamic performance of small spheres from subsonic to high supersonic velocities," *JAS*, vol. 12, no. 4, 1945.
5. M. P. Syshchikova, M. K. Berezkina, and A. N. Semenov, "Head shock-wave separation from a sphere in argon and nitrogen," collection: Aerophysical Investigations of Supersonic Flows [in Russian], Yu. A. Dunaev, ed., Izd-vo Nauka, 1967.
6. V. G. Maslennikov and A. M. Studenkov, "Position of the head shock wave at Mach numbers close to unity," collection: Aerophysical Investigations of Supersonic Flows [in Russian], Yu. A. Dunaev, ed., Izd-vo Nauka, 1967.
7. S. M. Gilinskii and M. G. Lebedev, "Investigation of low supersonic velocity flows with detached shock waves past plane and axisymmetric bodies," *Izv. AN SSSR, Mekhanika*, no. 1, 1965.

16 October 1967

Leningrad